ISSN 1070-3632, Russian Journal of General Chemistry, 2012, Vol. 82, No. 5, pp. 827–834. © Pleiades Publishing, Ltd., 2012.
Original Russian Text © E.V. Guseva, A.V. Sokolova, A.M. Saifutdinov, A.A. Naumova, V.K. Polovnyak, 2012, published in Zhurnal Obshchei Khimii, 2012, Vol. 82, No. 5, pp. 719–726.

Kinetics of Homogeneous Dehydrogenation of Formic Acid in the Presence of Supramolecular Rhodium(III) Complex with P-Functionalized Calix[4]resorcine

E. V. Guseva, A. V. Sokolova, A. M. Saifutdinov, A. A. Naumova, and V. K. Polovnyak

Kazan State Technological University, ul. K. Marksa 68, Kazan, 420015 Tatarstan, Russia
e-mail: leylaha@mail.ru

Received September 6, 2010

Abstract—The kinetics of homogeneous dehydrogenation of formic acid in the presence of supramolecular rhodium(III) complex with P-functionalized calix[4]resorcine were studied in dioxane, tetrahydrofuran, dimethylformamide, and binary formamide–dioxane mixtures (volume ratio 10 : 90, 20 : 80, 30 : 70) over a wide temperature range (40–90°C). The examined Rh(III) complex catalyzed the dehydrogenation process, and its catalytic activity was higher than that observed previously for rhodium complexes with non-macrocyclic phosphorus-containing ligands. The dehydrogenation rate constants were proportional to neither catalyst concentration nor dielectric constant of the medium, which is likely to be related to supramolecular nature of the Rh(III) complex. No micelle formation was observed in the examined systems.

DOI: 10.1134/S1070363212050040

In recent time new eco-friendly technologies capable of competing with natural catalytic systems have been developed. Potentially interesting are three-dimensional receptors based on calixresorcinarene scaffold, whose functionalization could give rise to catalytically active structures. For example, it is known [1, 2] that aminomethylated calix[4]resorcines catalyze hydrolysis of phosphorus acid esters.

Donor groups fixed at the upper or lower rim of a calix[4]resorcine can be involved in both inner- and outer-sphere coordination to metal ions. Such metal complex systems also exhibit catalytic activity in some processes [3]. These systems are obtained with the use of platinum metal compounds, in particular rhodium compounds, and their selectivity is com-parable with that of natural catalysts [4].

Rhodium(I) and rhodium(III) complexes with organo-phosphorus ligands are known [5–7] to catalyze homogeneous dehydrogenation of formic acid under atmospheric pressure at a temperature about 50°C. We previously synthesized complex **I**, octachloridotetra-dioxido{(4,6,10,12,16,18,22,24-octahydroxy-2,8,14,20-tetra[*p*-(diphenylphosphino)phenyl]pentacyclo[19.3.1.1^{3,7}.1^{9,13}.1^{15,19}]octacosa-1(25),3,5,7(28),9,11,13(27),15,17,19(26),21,23-dodecaene)}tetrarhodium(III) [8] from P(III)-functionalized calix[4]resorcine and triaqua trichloro rhodium complex. In the further treatment, compound **I** will be referred to as a structural unit with the composition L·4[$Rh^{+3}(O_2^-)(Cl^-)_2$], where L is P(III)-functionalized calix[4]resorcine. The present article reports on the results of our study on the kinetics of homogeneous dehydrogenation of formic acid in the presence of complex **I** and its catalytic activity as compared to rhodium complexes studied previously [5, 6]. Study on catalytic activity in this reaction is important from the viewpoint of understanding mechanisms of catalytic hydrogen liberation processes [5, 9–12].

Catalytic activity of highly organized systems based on calix[4]resorcines often depends on the type and properties of aggregates formed therein [1, 2]. Therefore, we also examined self-aggregation (self-association) of compound **I** in binary solvent consisting of formamide and dioxane in the range of concentrations $c_{\mathbf{I}}$ from 1×10^{-4} to 5×10^{-4} M in the presence and in the absence of formic acid. It is known [13, 14] that formamide is a strongly solvating solvent toward formic acid. By analogy with [5, 6, 13], binary solvent was used to estimate the effect of solvent polarity. The effect of specific solvation was estimated by measuring the reaction rate in dioxane, tetrahydrofuran (THF), and dimethylformamide (DMF).

Calix[4]resorcines exhibit surfactant properties and undergo self-organization to form micelles or lamellas, depending on the conformation. The catalytic activity

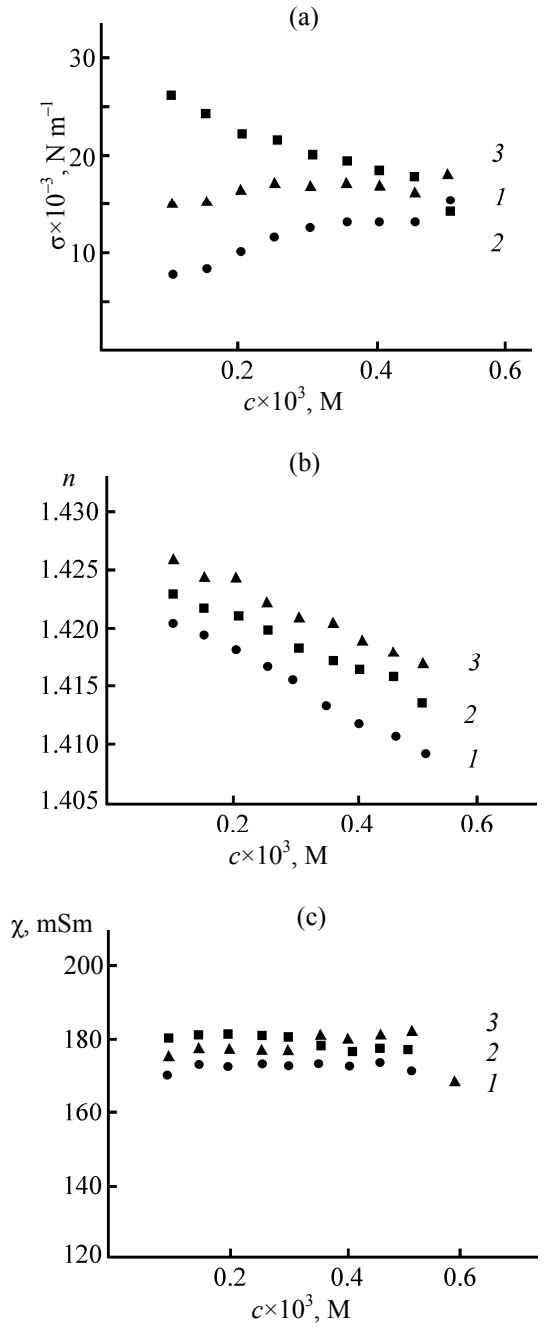

Fig. 1. Variation of the (a) surface tension, (b) refractive index, and (c) electric conductivity of compound **I**, depending on its concentration in formamide–dioxane mixtures at a ratio of (*1*) 10 : 90, (*2*) 20 : 80, and (*3*) 30 : 70 vol %.

of calix[4]resorcines is largely determined by the type of their aggregates and their properties [1, 2, 15]. It might be expected that metal complexes based on calix [4]resorcines also exhibit analogous properties, for the presence of multiply charged ions is known [16] to reduce critical micelle concentration.

The aggregation of **I** was studied by tensiometry [1, 2, 17, 18] at formamide–dioxane volume ratios of 10 : 90, 20 : 80, and 30 : 70 in the concentration range $c_{\mathbf{I}}$ 1×10^{-4}–5×10^{-4} M in the presence and in the absence of formic acid. The aggregation process in nonaqueous media can also be studied by analysis of concentration dependences of the refractive index of solution, $n = f(c)$ [19]. According to [19], variation of the structure of particles and aggregation are indicated by sharp change (bend) of the shape of the structure–property dependence. The dependences $\sigma = f(c)$ and $n = f(c)$ shown in Figs. 1a and 1b suggest the absence of aggregation of compound **I** under the given conditions. Therefore, the kinetic data were analyzed in terms of formal kinetic relations [20].

Decomposition of formic acid catalyzed by phosphine- and phosphite-containing Rh(I) and Rh(III) complexes is described by Eq. (1) [5, 6, 13].

$$HCOOH \xrightarrow{cat} H_2 + CO_2. \qquad (1)$$

Preliminary volumetric and chromatographic studies on catalytic decomposition of formic acid in the presence of complex **I** showed that the reaction stoichiometry conforms to Eq. (1). The reaction was of pseudofirst order in the catalyst [5, 6, 13, 20], for it was carried out with excess formic acid (c = 0.5 M). No appreciable decomposition of formic acid was observed in the presence of both components of complex **I**, ligand L and $RhCl_3 \cdot 3H_2O$, taken together or separately. Series of kinetic experiments were performed at different concentrations of **I** in binary formamide–dioxane mixtures with different compositions at different temperatures.

Measurement of electric conductivity of rhodium complexes with nonmacrocyclic phosphorus-containing ligands in different solvents revealed that these complexes almost do not undergo dissociation in dioxane–formamide mixtures [5, 6, 13]. Analogous results were obtained by measuring the conductivity of complex **I** in formamide–dioxane (Fig. 1c), so that the absence of dissociation of **I** was presumed. We believe that the reaction of formic acid with compound **I** follows the mechanism described previously in [5, 6, 13] and that the kinetics of decomposition of the transition complex formed by compound **I** with formate ion conforms to Eq. (2) provided that the reaction is carried out under pseudofirst-order conditions with respect to the catalyst.

$$W = k_{ap}[Rh]. \qquad (2)$$

Here, $k_{ap} = k$[HCOOH]. The experimental reaction rates were calculated using Eq. (3):

$$W = V/(2\tau \times 60 \times V_g)\ (\text{mol s}^{-1}). \quad (3)$$

Here, V is the overall volume of H_2 and CO_2 liberated over a period of time τ at given temperature and pressure; V_g is the volume of 1 mol of gas at a given temperature and atmospheric pressure. We also calculated the activity of catalytic centers (turnover frequency, TOF), which is equivalent to the first-order rate constant, using formula (4) [21].

$$\text{TOF} = n(\text{HCOOH})/[n(\text{cat})\,\tau]. \quad (4)$$

Here, n(HCOOH) is the amount of reacted formic acid molecules, mol; τ is the time, h; n(cat) is the number of active centers in the catalyst, mol: $n(\text{cat}) = 4\,m/M$, where m is the amount of compound **I**, g, M is its molecular weight, g mol^{-1}, and 4 is the number of rhodium atom in molecule **I**.

The kinetic parameters were calculated by substituting the experimental reaction rates into Eq. (2) and representing as TOF [Eq. (4)]. The energies of activation were determined by plotting the temperature dependences of TOF in the Arrhenius coordinates. The results are collected in Table 1.

The transformation of **I** during the process was monitored by electronic spectroscopy, electron spin resonance (ESR), and ^{31}P NMR. The electronic absorption spectra of metal complexes with macrocyclic ligands and dioxygen molecule typically contain a doublet band in the region λ 500–770 nm due to charge transfer from the metal to the ligand (MLCT) and a singlet $\sigma \rightarrow \sigma^*$ band [22–24]. Compound **I** displayed in the electronic absorption spectrum [8] a doublet at λ_{max} ~550/530 nm (MLCT), the $\sigma \rightarrow \sigma^*$ transition gave rise to a strong band at λ_{max} ~340 nm, a triplet band with λ_{max} ~440/410/380 nm was assigned to *d*–*d* transitions from the ground state to $^1T_{1g}$ and $^1T_{2g}$, and intraligand transitions were observed at λ_{max} ~285, 245, and 230–220 nm. The ESR parameters (g_1 = 2.103, g_2 = 2.028, g_3 = 1.974, $\langle g \rangle$ = 2.035) indicated rhombic symmetry and radical nature of the complex. Comparison of the electronic absorption spectra of reaction mixtures in the initial moment and in 10–30 min after the reaction started showed reduction of the intensity of *d*–*d* bands at λ 440, 410, and 380 nm to some value. The MLCT and $\sigma \rightarrow \sigma^*$ bands disappeared almost completely within the first 5 min. The ESR study revealed no paramagnetic species after 5–10 min. The ^{31}P NMR spectrum contained one phosphorus signal at δ_P 26.12 ppm, which indicated that elimination of ligand molecule did not occur in the course of homogeneous dehydrogenation. When the reaction was complete, excess formic acid and the solvent were removed in a stream of argon; the electronic absorption, ESR, IR, Raman, and ^{31}P NMR spectra of the light brown compound thus isolated were identical to the corresponding parameters of initial complex **I** [8].

The time dependence of the volume of liberated gases was typical of catalytic processes following pseudofirst- order kinetics with respect to the catalyst. Such dependences at different temperatures are shown in Fig. 2. Analysis of the temperature dependences of the rate constants (TOF) at different concentrations of **I** and different compositions of the medium (Fig. 3) revealed the following relations. The catalytic activity (TOF) of **I** at $c = 1.0 \times 10^{-4}$ M increases with rise in solvent polarity. At $c = 5.0 \times 10^{-4}$ M, the catalytic activity of **I** is almost independent of the solvent polarity. At $c = 2.5 \times 10^{-4}$ M, the catalytic activity of **I** increases until the concentration of formamide reaches 20 vol % and then remains constant.

In formamide–dioxane at a volume ratio of 10 : 90, TOF increases with rise in both concentration of **I** and temperature (Fig. 3a). In binary mixtures containing 30 vol % of formamide, higher catalytic activity is observed at lower concentration (Fig. 3c) but at higher temperature. The catalytic activity of **I** in formamide–dioxane (20 : 80 vol %; $c_{\mathbf{I}} = 2.5 \times 10^{-4}$ M) sharply increases as the temperature changes from 40 to 60°C, whereas further rise in temperature is accompanied by slower increase of TOF (Fig. 3b).

From the practical viewpoint, it is more advantageous to use lower concentrations and lower temperatures in catalytic processes. Therefore, our subsequent experiments were carried out under the following (optimal) conditions: temperature 60°C; concentration $c_{\mathbf{I}} = 2.5 \times 10^{-4}$ M; solvent formamide–dioxane (20 : 80 by volume). Taking into account that the composition of binary solvent affects the reaction rate, we examined the dependence of the catalytic activity of complex **I** on the polarity of the medium at $c_{\mathbf{I}} = 2.5 \times 10^{-4}$ M (Table 2). Increase in the fraction of formamide in its mixture with dioxane, i.e., increase in the dielectric constant ε of the medium, is accompanied by increase in the energy of activation E_{TOF}; however, the largest TOF was observed in the solvent containing 20 vol % of formamide. No analogous relation between TOF and ε was observed in pure dioxane, THF, or DMF. Among pure solvents, the

Table 1. Kinetic and activation parameters of catalytic dehydrogenation of formic acid under different conditions

Parameter[a]	40°C	50°C	60°C	70°C	80°C	90°C
Formamide–dioxane (10 : 90 vol %); ε = 14.00; c = 1.0×10^{-4} M; E_{TOF} = 6.993 kJ mol^{-1}						
TOF, h^{-1}	3.6	27.1	37.1	53.3	75.0	128.4
τ, min	120.0	120.0	120.0	120.0	120.0	120.0
Formamide–dioxane (20:80 vol %); ε 24.75; c 1.0×10^{-4} M; E_{TOF} 7.834 kJ mol^{-1}						
TOF, h^{-1}	19.9	222.4	412.3	515.3	716.0	1079.5
τ, min	120	20	20	20	20	20
Formamide–dioxane (30:70 vol %); ε 34.50; c 1.0×10^{-4} M; E_{TOF} 9.442 kJ mol^{-1}						
TOF, h^{-1}	126.6	450.6	634.7	3075.7	5365.3	4394.8
τ, min	6.0	13.0	20	20	20.0	13.0
Formamide–dioxane (10:90 vol %); ε 14.00; c 2.5×10^{-4} M; E_{TOF} 5.352 kJ mol^{-1}						
TOF, h^{-1}	56.4	217.0	376.1	538.1	555.5	764.8
τ, min	20.0	4.0	6.0	5.0	10.0	16.0
Formamide–dioxane (20:80 vol %); ε 24.75; c 2.5×10^{-4} M; E_{TOF} 6.073 kJ mol^{-1}						
TOF, h^{-1}	120.9	1620.1	3185.2	2725.3	3191.8	3107.1
τ, min	14.0	12.0	20.0	15.0	20.0	20.0
Formamide–dioxane (30:70 vol %); ε 34.50; c 2.5×10^{-4} M; E_{TOF} 7.044 kJ mol^{-1}						
TOF, h^{-1}	89.5	889.6	1089.2	989.4	3065.9	3107.1
τ, min	16.0	20.0	20.0	20.0	20.0	20.0
Formamide–dioxane (10: 90 vol %); ε 14.00; c 5.0×10^{-4} M; E_{TOF} 3.836 kJ mol^{-1}						
TOF, h^{-1}	151.9	530.4	634.2	905.9	935.9	1017.6
τ, min	2.0	9.0	13.0	8.0	15.0	20.0
Formamide–dioxane (20:80 vol %); ε 24.75; c 5.0×10^{-4} M; E_{TOF} 5.910 kJ mol^{-1}						
TOF, h^{-1}	21.7	764.4	802.8	911.3	1323.6	490.1
τ, min	11.0	13.0	10.0	11.0	12.0	17.0
Formamide–dioxane (30:70 vol %); ε 34.50; c 5.0×10^{-4} M; E_{TOF} 5.207 kJ mol^{-1}						
TOF, h^{-1}	57.2	419.7	682.8	648.8	841.1	927.1
τ, min	12.0	11.0	9.0	12.0	13.0	14.0

[a] τ is the time necessary to attain the maximal TOF value.

largest TOF was observed in dioxane, but E_{TOF} was also high.

Thus, the solvent effect cannot be interpreted in terms of the polarity of the medium, i.e., it is specific.

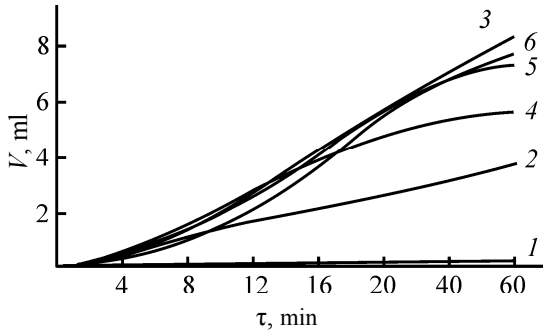

Fig. 2. Kinetics of gas evolution (H_2 + CO_2) in the catalytic dehydrogenation of formic acid in the presence of complex **I**; $c_{\mathbf{I}}$ = 2.5 × 10^{-4} M, formamide–dioxane ratio 20 : 80 vol %; temperature, °C: (*1*) 40, (*2*) 50, (*3*) 60, (*4*) 70, (*5*) 80, and (*6*) 90.

Presumably, acceleration of the reaction in the presence of formamide results from solvation of formic acid by formamide [13].

It was found previously that formate ion replaces one chloride ion in the coordination sphere of rhodium complexes with phosphorus-containing non-macrocyclic ligands at the stage preceding the rate-determining stage [5, 13].

$$RhClCO(PPh_3)_2 + HCOOH \rightarrow RhCO(PPh_3)_2HCOO + HCl. \quad (5)$$

We also examined how addition of chloride ions (as sodium chloride) affects the rate of decomposition of formic acid. The concentration ratio of chloride ions and compound **I** was varied from 1 : 2.5 to 15 : 1 (Table 3). When the concentration of Cl^- was higher than or equal to the concentration of **I**, the reaction slowed down. A small gain in the reaction rate with

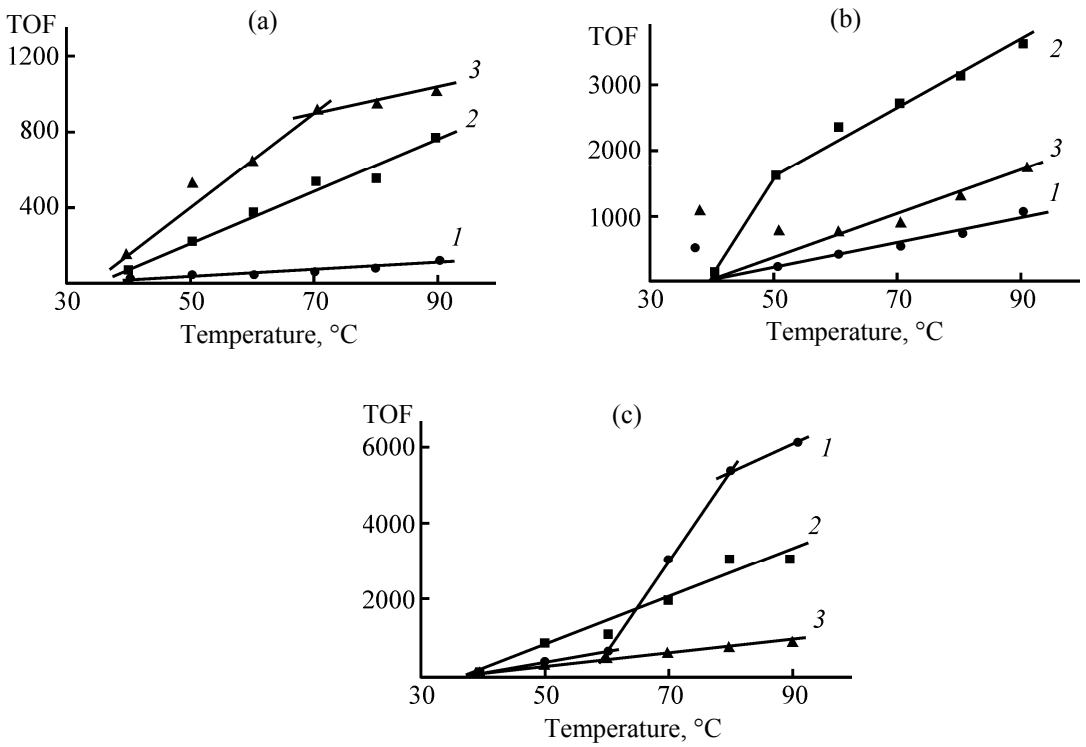

Fig. 3. Temperature dependence of TOF for catalytic dehydrogenation of formic acid in the presence of complex **I**; formamide–dioxane ratio (a) 10 : 90, (b) 20 : 80, and (c) 30 : 70 vol %; concentration of **I**: (*1*) 1.0×10^{-4}, (*2*) 2.5×10^{-4}, and (*3*) 5.0×10^{-4} M.

rise in chloride ion concentration in the range from 2.5×10^{-4} to 37.5×10^{-4} M is likely to result from variation of ionic strength of the solution. At a chloride ion concentration lower than that of compound **I** the reaction rate W was appreciably higher than in the first case but lower than in the absence of chloride ions. Taking into account the data given in Table 3 and those reported in [5, 6, 13], concluded that the addition of formate ion to complex **I** involves elimination of chloride ion from the metal coordination sphere. The presence of an additional amount of chloride ions hampers coordination of formate ions at the stages preceding the rate-determining stage, which is responsible for the observed inhibition.

It was interesting to compare the catalytic activity of complex **I** in homogeneous dehydrogenation of formic acid with the catalytic activity of Rh(I) and Rh(III) complexes containing phosphine and phosphite ligands but no calixresorcinarene matrix [5, 6, 12, 25]. The data given in Table 4 indicate higher catalytic activity of **I**. A probable reason is the ability of **I** to bind dioxygen and participate in transfer of one or two electrons via electron density redistribution between the coordination center and calixresorcinarene matrix.

EXPERIMENTAL

Compound **I** was synthesized according to the procedure described in [8]. Sodium chloride and rhodium(III) chloride trihydrate ($RhCl_3 \cdot 3H_2O$) of

Table 2. Effect of solvent polarity on the kinetic parameters of the reaction $HCOOH \rightarrow H_2 + CO_2$; concentration of **I** $c_{\mathbf{I}} = 2.5 \times 10^{-4}$ M

Solvent (ratio, vol %)	ε	T, °C	TOF, h^{-1}	τ, min	E_{TOF}, kJ mol^{-1}
Formamide–dioxane					
10:90	14.00	50	217.0	4.0	5.352
		60	376.1	6.0	
20:80	24.75	50	1620.1	12.0	6.073
		60	3185.2	20.0	
30:70	34.50	50	889.6	20.0	7.044
		60	1089.2	20.0	
Dioxane	2.21	50	470.8	20.0	8.271
		55	665.4	18.0	
		60	1016.4	19.0	
THF	7.39	25	299.8	11.0	4.696
		30	364.5	15.0	
		40	630.4	19.0	
DMF	37.6	50	230.0	20	8.898
		55	401.4	20	
		60	525.3	19	

Table 3. Effect of chloride ions on the rate of decomposition of formic acid in formamide–dioxane (20 : 80 vol %); temperature 60°C; concentration of **I** $c_{\mathbf{I}} = 2.5 \times 10^{-4}$ M

Concentration of NaCl, M	$W \times 10^{10}$, mol s^{-1}
–	735
1.0×10^{-4}	167.5
2.5×10^{-4}	20.6
7.5×10^{-4}	20.8
37.5×10^{-4}	21.6

analytically pure grade were used. The solvents were purified and dehydrated by standard procedures just before use. Each experiment was repeated in triplicate. The surface tension of solutions of **I** was determined by the Du Noüy ring method using a VT type torsion balance [17, 18]. The refractive indices were measured with the aid of an IRF-22 refractometer. The electric conductivities were measured at 25°C on an LM-301 conductometer equipped with an LM-3000 standard cell. The temperature was maintained constant with an accuracy of ±0.1°C.

Dehydrogenation of formic acid was performed according to the procedure described in [5, 6, 13]. The reaction was carried out in a hermetically closed cell maintained at a constant temperature (Fig. 4); the cell was connected to a pressure gage and was equipped with a gas sampling device. The pressure gage case was maintained at 25.0 ± 0.1°C. The cell was purged with argon over a period of 5–10 min, charged with 20 ml of a formamide–dioxane mixture at a volume ratio of 10 : 90, 20 : 80. or 30 : 70, and purged again with argon over a period of 5–10 min. A required amount of compound **I** was added to a concentration $c_{\mathbf{I}}$ of 1.0×10^{-4}, 2.5×10^{-4}, or 5.0×10^{-4} M, stirring was started, and the solution was purged with argon, the completeness of oxygen removal being monitored by chromatography using a Varian 3700 instrument (carrier gas nitrogen, stationary phase Carboxen 1000, thermal conductivity detector). The stirring was turned off, formic acid was added with a syringe to a concentration of 0.5 M, and the stirring was turned on. This moment was taken as reaction onset. The reaction rate was measured by the water level in the burette, which was equal to the volume of liberated gases (H_2 and CO_2). The water in the burette was acidified with hydrochloric acid to a pH value corresponding to the first dissociation constant of H_2CO_3 to avoid absorption of CO_2 by water. The solubility of hydrogen in acidified water was also sharply reduced. Thus the volume of liberated hydrogen or carbon dioxide is equal (within the experimental error) to the half volume of water expelled from the burette. Isolation of the products was also controlled by chromatography (Varian 3700, carrier gas nitrogen, stationary phase

Table 4. Kinetic parameters of dehydrogenation of formic acid in the presence of different catalysts

Catalyst, solvent (ratio, vol %)	$c_{\mathbf{I}} \times 10^3$, M	Temperature, °C	$k_{ap} \times 10^3$, s^{-1}	E_a, kcal mol^{-1}	TOF, h^{-1} (τ, [a] min)
$RhClCO[P(OPr\text{-}i)_3]_2$, Formamide–dioxane (10 : 90)	1.0–2.5	50	0.26	14.0±0.3	148.5 (65)
$Rh_2Cl_2[P(OPr\text{-}i)_3]_4$, Formamide–dioxane (10 : 90)	1.0–2.5	50	4.3	24.8±0.7	412.6 (20)
$Rh_2Cl_2[P(OR)_2OH]_4$, Formamide–dioxane (10 : 90)	1.0–2.5	50	5.1–5.3	23.8–24.2	–
$RhClCO(PPh_3)_2$, Formamide–dioxane (10 : 90)	400–600	50	0.05	19.4±0.4	–
$Rh_2Cl_6[P(OEt)_3]_4$, Formamide–dioxane (10 : 90)	1.0–2.5	40	3.84	–	302.2 (15)
$RhCl_3 \cdot xH_2O$, $HCOOH/NEt_3$	–	40	–	–	~3 (360)
$[Rh(C_6H_4PPh_2)(PPh_3)_2]$, toluene	–	20	0.0006	–	–
Compound **I**, Formamide–dioxane (20 : 80)	0.25	60	14.7	5.5	2186 (20)

[a] See note "a" to Table 1.

Carboxen 1000, thermal conductivity detector). The transformation of compound **I** during the process was monitored by electronic spectroscopy (SF-16 spectrophotometer, λ range 200–350 nm; Specol, λ 350–700 nm; cell path length 1 cm, concentration 1×10^{-3} M), electron spin resonance (Radiopan SE/X-2544), and ^{31}P NMR (Bruker MSL-400, 166.93 MHz, 85% H_3PO_4 as external reference).

The effect of chloride ions on the reaction rate was studied by plotting kinetic curves at Cl^--to-**I** concentration ratios of 1 : 2.5, 1 : 1, 3 : 1, and 15 : 1.

Complex **I** isolated after the reaction completion was analyzed for carbon and hydrogen using a Carlo Erba EA 1108 CHN analyzer; the phosphorus content was determined by photocolorimetry using an FEK-56M-U4-2 photocolorimeter; the rhodium content was determined by the X-ray fluorescence method (SUR-02 RENOM F1); the concentration of chlorine was determined according to [26]. The melting point of complex **I** isolated after the reaction was determined from the TG and DTG curves obtained on a Q-1500D Paulik–Paulik–Erday derivatograph (sample weight 50–60 mg, heating rate 10 deg/min). The IR spectra of crystalline samples dispersed in anhydrous mineral oil were recorded on UFS 113-V (600–200 cm^{-1}) and Bruker Vector 22 spectrometers (4000–450 cm^{-1}) with Fourier transform. The ESR spectra were measured on a Radiopan SE/X-2544 spectrometer (300 K, 9.020 GHz, crystalline sample). The ^1H and ^{31}P NMR spectra were obtained on a Bruker MSL-400 instrument at 400.13 and 166.93 MHz, respectively; the chemical shifts were measured relative to the residual proton signal of the solvent (^1H) or 85% H_3PO_4 (^{31}P).

The properties of compound **I** isolated after the reaction was complete, were similar to those reported in [8]: mp 250°C (decomp.). IR spectrum, ν, cm^{-1}: 3180 (O–H); 3061 (CH_{arom}), 2854 (CH), 1599 (C–C_{arom}), 1403 (δ CH), 1305 (P–C_{arom}), 1118, 1157, 1160 (δ P–C_{arom}, δ C–C_{arom}, C–C, CH, C_{arom}–O); 1027 (O–O); 1087, 1017, 997, 975 (δ P–C_{arom}, δ C–C_{arom}, CH, C–C, C_{arom}–O); 845, 834 (δ Ph, COC, C–C); 803 (P–C_{arom}); 750, 693, 617 (δ Ph); 538, 420 (δ P–C_{arom}, macroring); 266, 253, 225, 215, 205 (δ PPh_2, macroring); 335 (Rh–Cl); 305, 282 (Rh–P). Electronic absorption spectrum (methanol or formamide–dioxane), λ, nm: 220–230, 245, 285, 340, 380, 410, 440, 530, 550. ^{31}P NMR spectrum: δ_P 26.12 ppm, $^1J_{Rh-P}$ = 208 Hz. ESR spectrum: g_1 = 2.103, g_2 = 2.028, g_3 = 1.974, $\langle g \rangle$ = 2.035. The calixresorcinarene fragment in complex **I** retains its *chair* conformation, as follows from the positions of signals from conformation-dependent protons in the ^1H NMR spectrum (DMSO-d_6), δ, ppm: 5.77 s and 5.78 s (2H each, *o*-H), 5.83 s and 5.92 s (2H each, *m*-H). Found, %: C 51.03; H 3.28; Cl 12.10; P 5.22; Rh 17.92. $C_{100}H_{76}Cl_8O_{16}P_4Rh_4$. Calculated, %: C 51.00; H 3.20; Cl 12.07; P 5.20; Rh 17.50.

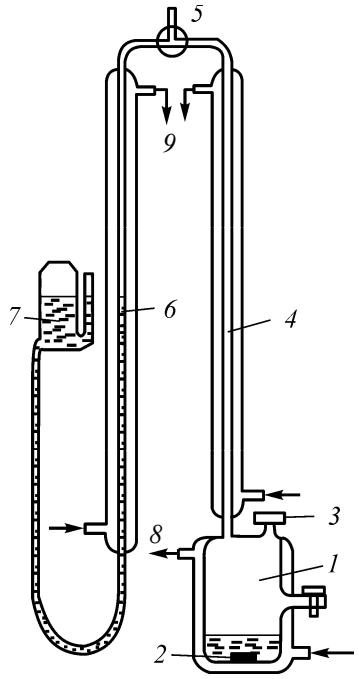

Fig. 4. Setup for homogeneous dehydrogenation of formic acid: (*1*) thermostatted cell, (*2*) magnetic stirrer, (*3*) sampling arm, (*4*) thermostatted capillary, (*5*) three-way stopcock, (*6*) gas burette, (*7*) elevated reservoir, and (*8*, *9*) heating agent.

REFERENCES

1. Ryzhkina, I.S., Babkina, Ya.A., Lukashenko, S.S., Enikeev, K.M., Kudryavtseva, L.A., and Konovalov, A.I., *Izv. Ross. Akad. Nauk, Ser. Khim*., 2002, no. 12, p. 2026.
2. Ryzhkina, I.S., Kudryavtseva, L.A., Babkina, Ya.A., Enikeev, K.M., Pudovik, M.A., and Konovalov, A.I., *Izv. Ross. Akad. Nauk, Ser. Khim*., 2000, no. 18, p. 1361.
3. Karakhanov, E.A., Maksimov, A.L., and Runova, E.A., *Usp. Khim*., 2005, vol. 74, no. 1, p. 104.
4. Collman, J.P., Hegedus, L.G., Norton, J.R., and Finke, R.G., *Principles and Applications of Organotransition Metal Chemistry*, Mill Valley, CA: University Science Books, 1987.
5. Yurtchenko, E.N. and Anikeenko, P.P., *React. Kinet. Catal. Lett*., 1975, vol. 2, p. 65.
6. Gracheva, L.S., *Cand. Sci. (Chem.) Dissertation*, Kazan, 1978.
7. Yurchenko, E.N., Gracheva, L.S., Al't, L.Ya., and

Pavlyukhina, L.A., *Koord. Khim*., 1981, vol. 7, no. 6, p. 930.

8. Guseva, E.V., Morozov, V.I, Karimova, D.T, Gavrilova, E.L., Naumova, A.A., Polovnyak, V.K., and Krasil'nikova, E.A., *Russ. J. Gen. Chem*., 2010, vol. 80, no. 1, p. 47.
9. Elizarova, G.L., Matvienko, L.G., and Yurchenko, E.N., USSR Inventor's Certificate no. 454 763, 1979; *Byull. Izobret*., 1979, no. 6.
10. Forster, D. and Beck, G.R., *J. Chem. Soc. D*, 1971, p. 1072.
11. Gan, W., Dyson, P.J., and Laurenczy, G., *React. Kinet. Catal. Lett*., 2009, vol. 98, p. 205.
12. Fukuzumi, S., Kobayashi, T., and Suenobu, T., *Chem. Sus. Chem*., 2008, vol. 1, no. 10, p. 827.
13. Yurchenko, E.N., *Kinet. Katal*., 1973, vol. 14, no. 2, p. 515.
14. Fialkov, Yu.Ya., *Rastvoritel' kak sredstvo upravleniya khimicheskim protsessom* (Solvent as a Tool for Controlling Chemical Process), Leningrad: Khimiya, 1990.
15. Steed, J.W. and Atwood, J.L., *Supramolecular Chemistry*, Chichester: Wiley, 200.
16. Amirov, R.R., *Soedineniya metallov kak magnitno-relaksatsionnye zondy dlya vysokoorganizovannykh sred* (Metal Compounds as Magnetic Relaxation Probes for Highly Organized Media) Kazan: Novoe Znanie, 2005.
17. *Poverkhnostno-aktivnye veshchestva. Spravochnik* (Surfactants Handbook), Abramzon, A.A. and Gaevoi, G.M., Eds., Leningrad: Khimiya, 1979.
18. Pidwell, A.D., Collinson, S.R., Coles, S.J., Hursthouse, M.B., Schröder, M., and Bruce, D.W., *Chem. Commun*., 2000, p. 955.
19. Frolov, Yu.G., *Kurs kolloidnoi khimii. Poverkhnostnye yavleniya i dispersnye sistemy* (Lectures on Colloid Chemistry. Surface Phenomena and Disperse Systems), Moscow: Khimiya, 1988.
20. Denisov, E.T., *Kinetika gomogennykh khimicheskikh reaktsii* (Kinetics of Homogeneous Chemical Reactions), Moscow: Vysshaya Shkola, 1988.
21. Hagen, J., *Industrial Catalysis: A Practical Approach*, Weinheim: Wiey, 2006.
22. McEwen, Ch.N. and Rudat, M.A., *J. Am. Chem. Soc*., 1979, vol. 101, no. 21, p. 6472.
23. Wayland, B.B. and Newman, A.R., *Inorg. Chem*., 1981, vol. 20, no. 9, p. 3093.
24. Lever, E., *Inorganic Electronic Spectroscopy*, Amsterdam: Elsevier, 1984, 2nd ed.
25. Strauss, S.H., Whitmire, K.H., and Shriver, D.F., *J. Organomet. Chem*., 1979, vol. 174, p. 59.
26. *Metody kolichestvennogo organicheskogo elementnogo mikroanaliza* (Methods of Quantitative Organic Elemental Microanalysis), Gel'man, A.I., Ed., Moscow: Khimiya, 1987, p. 230.